Electrical discharge surface texturing for enhanced pool boiling heat transfer

Gurpyar Dhadda[1,2], Mohamed Hamed[1,2], Philip Koshy[2,*]

[1]Thermal Processing Laboratory, [2]Department of Mechanical Engineering
McMaster University, Hamilton, Canada

*Corresponding author: koshy@mcmaster.ca

Abstract

This research pertains to pool boiling heat transfer characteristics of Aluminum 6061 alloy surfaces that were textured using sink electrical discharge machining (EDM). Prior related work elsewhere utilized EDM as an essential means to roughen a surface or fabricate geometric features such as microchannels and micropillars to investigate boiling. As opposed to this, the present work systematically examined the effect of EDM process parameters viz., the discharge current and the discharge duration to enhance/benchmark boiling performance in the natural convection and nucleate boiling regimes and comprehend underlying mechanisms. A process-related factor that limits boiling was found to be the growth of a superficial layer on the machined surface, the formation of which is facilitated by the hydrocarbon dielectric fluid used in EDM. This notwithstanding, the highest heat transfer coefficient obtained in this work was roughly five times as that of a reference polished surface. The Data Dependent Systems methodology was adopted to mathematically extract characteristic crater geometry from EDM-textured surface profiles, which highlighted the significance of parameters that are physically relevant such as the crater diameter and the crater volume in correlating boiling performance.

Keywords

Electrical discharge machining, Heat transfer enhancement, Pool boiling, Surface topography

Nomenclature

Abbreviations

DDS	Data Dependent System
EDM	Electrical Discharge Machining
MAE	Mean Absolute Error
ONB	Onset of Nucleate Boiling

Symbols

C_d	diameter of characteristic crater (μm)
C_h	depth of characteristic crater (μm)
h	heat transfer coefficient (kW/m^{2}K)
i_e	discharge current (A)
q"	surface heat flux (kW/m^2)
Ra	average roughness (μm)
Rku	kurtosis of profile
Rq	root mean squared roughness (μm)

42	Rsk	skewness of profile
43	Rz	maximum profile depth (μm)
44	t_e	discharge duration (μs)
45	T_s	wall surface temperature (°C)
46	T_{sat}	saturation temperature (°C)
47	$\Delta T_{s\text{-}ONB}$	wall superheat at onset of nucleate boiling (°C)
48	ΔT_{sat}	wall superheat (°C)
49	u_i	open circuit voltage (V)
50	u_e	discharge voltage (V)
51	V_c	volume of characteristic crater (μm^3)

1. Introduction

Nucleate pool boiling is widely taken advantage of in devising compact heat exchangers for passive thermal management in high heat flux applications. This mode of heat transfer involves both the latent and sensible heats of the coolant, which facilitates significantly higher heat dissipation relative to free or forced convection. In the case of water, for instance, the latent heat of vaporization is more than two orders of magnitude higher than the sensible heat.

Noting that bubbles tend to nucleate from surface flaws such as cavities, further enhancements in pool boiling heat transfer may be achieved by altering the topography of the surface across which heat is transferred. This has resulted in the development of several engineered surfaces spanning the macroscale to the nanoscale, specifically conceived to bring about an increase in the density of bubble nucleation sites for intensified boiling, as reviewed by Liang and Mudawar (2019). This translates into a favourable decrease in the degree of surface superheat required for boiling incipience, as well as an increase in the heat transfer coefficient. One avenue to engineering a functional boiling surface is selective removal of material by machining. This paper details research on the application of electrical discharge machining (EDM) to tailor the topography of a surface towards enhancing its pool boiling performance.

EDM is a precision material removal process that utilizes the heat generated from controlled, rapid electrical spark discharges as detailed by Kunieda et al. (2005). The tool and workpiece electrodes are separated by a small gap of several tens of μm filled with a dielectric fluid (typically a hydrocarbon oil or deionized water), across which the discharges are struck. Machining progresses under a servo-controlled tool feed by repeated removal of small volumes

of material by melting and vaporization. The process primarily entails two configurations: sink EDM which involves shape replication using three-dimensional tooling, and wire EDM wherein swept surfaces are generated using a wire as the tool electrode. The process is commonly used in the tool and die, aerospace and medical industries.

A single discharge in EDM entails several distinct stages, which may be understood in terms of the corresponding segments in the voltage and current waveforms, shown schematically in Fig. 1a and 1b, respectively. Increasing the voltage to the open circuit voltage u_i (from 1 to 2) initiates ionization of the dielectric fluid in the machining gap (Fig. 1c). Ionization continues to proceed from 2 to 3, eventually leading to the breakdown of the dielectric fluid and the formation of a plasma channel across the inter-electrode gap (Fig. 1d). This results in the flow of current i_e (4 to 5) that corresponds to a drop in the voltage from the open circuit voltage to the discharge voltage u_e, which is typically around 20 V. The discharge is maintained for a period t_e known as the discharge duration, during which time, there is melting and vaporization of both the tool and the workpiece, and a gas bubble is formed around the plasma channel from vaporization of the dielectric fluid in the immediate vicinity. Terminating the voltage pulse from 5 to 6 stops the flow of the current, at which point the plasma channel implodes. The gas bubble collapses subsequently, which facilitates the removal of the molten material from the electrode surfaces in the form of microscopic debris (Fig. 1e). This cycle is repeated after a set pause-time. The process is designed to realize preferential material removal from the workpiece relative to the tool.

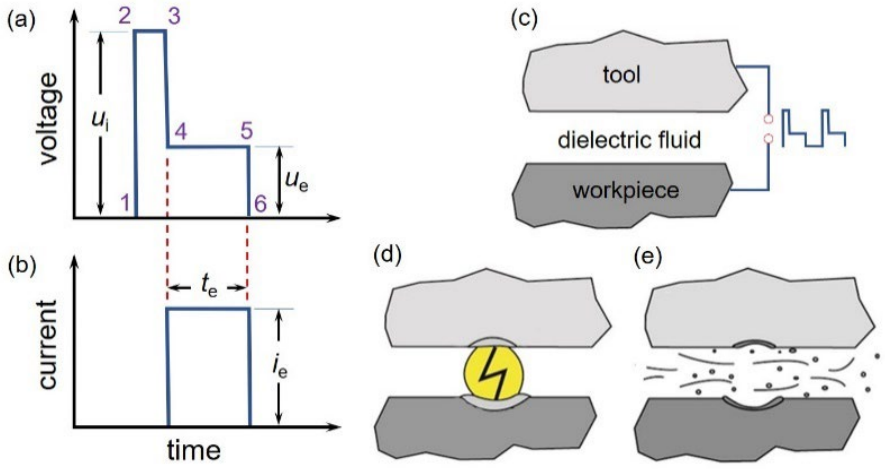

Fig. 1. Principle of electrical discharge machining.

The primary consideration in having adopted EDM as the means of texturing a surface to enhance boiling performance in this research is that the height distribution of the surface generated in EDM (Fig. 2a) is typically skewed to the right (positive skewness, Fig. 2b) as opposed to being Gaussian, as described by Stout et al. (1990). This implies that the surface profile comprises relatively few peaks interspersed among wide valleys (Fig. 2c), and that the surface presents many dimple-shaped, microscopic cavities. This is a consequence of the material being removed by the collective action of individual discharges. Such surface cavities may be supposed to be ideally suited to serve as bubble nucleation sites; besides, the size and aspect ratios of these cavities that have a critical influence on boiling may be manipulated by appropriately varying the discharge current i_e and the discharge duration t_e. Furthermore, surfaces machined using EDM in a hydrocarbon dielectric fluid have recently been shown by Guo et al. (2019) to be inherently hydrophobic. This is significant in this instance, given that unwetted surface cavities are favourably disposed towards nucleating bubbles due to their propensity to trap vapor embryos, as are micro-cracks that are typically induced during EDM.

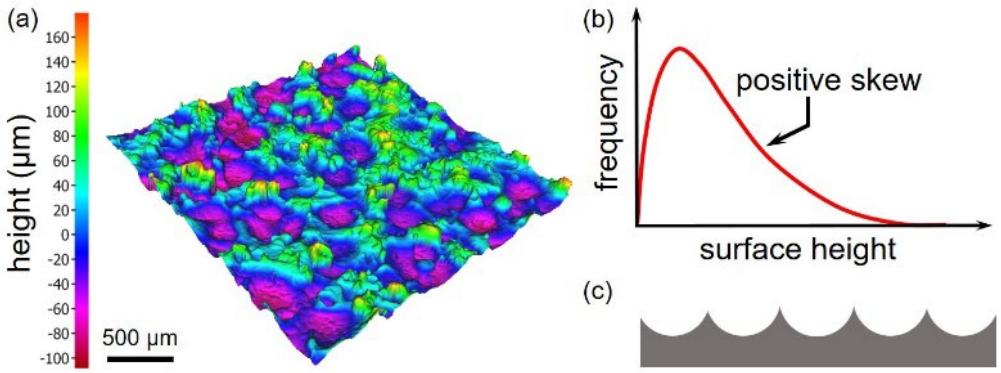

Fig. 2. Topography of EDM surfaces.

Such a texturing application of EDM is intriguing also from the machining perspective since the material removal rate in EDM is generally lower than that of conventional machining processes. Considering that texturing entails the removal of just a thin layer of material on the order of only several tenths of a mm in thickness, the said low removal rate of EDM is essentially irrelevant. Any undesirable metallurgical modification to the machined surface and surface cracks arising from the thermal nature of EDM are as well of little consequence in this application given that it is not load-bearing. Recent surface engineering applications of EDM elsewhere include the development of coatings of several mm thickness on electrically conducting substrates by Ahmed et al. (2020), and the enhancement of adhesive joining by Bangash et al. (2020).

There are just a handful of papers in the literature on the use of EDM for fabricating surfaces to enhance nucleate pool boiling performance. Wire EDM was used by Rahman and McCarthy (2017) to fabricate microchannels to investigate the influence of length scales in boiling; similarly, it was applied by Nirgude and Sahu (2017) to create surfaces comprising micro-pillars to enhance boiling performance. In these works, EDM was specifically used as a precision micro-machining process to generate structured surfaces with defined macro-geometric features,

rather than to exploit the unique topographic characteristics of EDM surfaces (highlighted in Fig. 2). During an investigation on confinement-driven pool boiling enhancement by Giesler and Bar-Cohen (2005), microchannels machined on aluminium surfaces using EDM were found to correspond to a better boiling performance relative to those finished using 400- and 600-grit abrasive paper. This work did not delve into any details of the EDM process, other than the mention of it having been used to machine the channels.

A research examining the influence of surface roughness on pool boiling heat transfer by Jones et al. (2009) used EDM to fabricate rough surfaces for comparison against a baseline polished surface. For water as the working fluid, this work indicated an EDM surface of roughness 10 μm *Ra* to correspond to a 100% increase in the heat transfer coefficient and a 6 °C decrease in the surface superheat for boiling incipience, relative to a polished surface. Boiling curves referring to EDM surfaces of roughness 1.1, 2.2 and 5.9 μm *Ra* were found to cluster together in this work, and to perform intermediate between the polished surface and the roughest EDM surface (10 μm *Ra*). Optical profilometry showed the actual area of EDM surfaces in contact with the fluid to be similar, and hence be unrelated to this behaviour. High-speed imaging indicated the EDM surfaces to correspond to a higher number of active nucleation sites, a higher bubble emission frequency and a smaller bubble departure diameter, as compared to a polished surface; however, the relatively strong performance of the EDM surface with a roughness of 10 μm *Ra* could not be clarified. Besides, although the performance improved significantly with an increase in roughness from 5.9 μm *Ra* to 10 μm *Ra*, surfaces with an even higher roughness were not investigated.

In studies by Giesler & Bar-Cohen (2005) and Jones et al. (2009), the research emphasis was on the application of EDM as an essential means to increasing the roughness of a functional boiling surface. The surfaces were characterized just in terms of their numerical roughness indices, with no consideration of the EDM process parameters themselves. In principle, a given value of a surface roughness parameter could be obtained by different combinations of discharge current and discharge duration in EDM; they would but refer to entirely different surface topographic characteristics, which in turn would correspond to boiling characteristics that are likely as different.

In the context of the relevant state-of-the-art reviewed above, the present work was embarked on to systematically investigate the boiling performance of EDM surfaces with respect to the discharge current and the discharge duration that are key process parameters in EDM. Emphasis was placed on identifying and understanding process-related factors that limit boiling, and to benchmark and maximize the boiling performance of EDM surfaces in the natural convection and nucleate boiling regimes. Additionally, boiling performance was correlated to several surface characteristic parameters.

2. Experimental

To the end of meeting the objectives above, surfaces were fabricated using sink EDM by systematically varying the discharge current i_e and discharge duration t_e over a wide range, using Aluminium 6061 as the work material. The open circuit voltage u_i was fixed at 100 V, and the process corresponded to a duty factor of 0.5. Cylindrical test blocks of 25.4 mm diameter were textured on one of the end-faces by removing material to a nominal depth of 0.15 mm using

168 copper electrodes, employing a tool-positive polarity and jump flushing of the dielectric fluid.
169 Machining predominantly involved a hydrocarbon oil as the dielectric fluid, with a few
170 complementary experiments using deionised water instead. The topography of machined
171 surfaces was characterized using an optical confocal microscope or a tactile profilometer.

172 Fig. 3 is a schematic diagram of the pool boiling vessel, showing only the most essential
173 elements for clarity; more details on the test setup, and on the calculation of heat flux and surface
174 temperature can be found in Dhadda (2019) and Ahmed & Hamed (2012). Three 250 W
175 cylindrical heat cartridges of 38.1 mm length and 6.35 mm diameter were mounted at the bottom
176 of the test block to heat the boiling surface under atmospheric pressure. The temperature
177 distribution in the test block was obtained using three Type-E thermocouples embedded in it, at
178 distances of 5, 10 and 15 mm from the top surface and distributed radially at 120° intervals at a
179 depth of 6 mm from the peripheral surface. Deionised water (4 L) was used as the working fluid
180 after degassing it using immersed heaters for 30 minutes before each experimental run. The pool
181 of water was maintained at the saturation temperature T_{sat} of 100 °C using bulk fluid heaters and
182 a condensing coil.

183 Boiling curves were obtained by increasing the power input to the test block and calculating the
184 wall heat flux and surface temperature from the temperatures measured within the test block at
185 steady state. Numerical simulation indicated the temperature distribution to be uniform across
186 the test surface. Heat loss from the test block was minimized by insulating it and heating the air
187 around it by using a guard heater. Bubble incipience and growth over the boiling surface was
188 visualized using a high-speed camera at 3000 frames per second. Undesirable bubble nucleation
189 around the periphery of the test block was minimized by applying an epoxy layer between the

test coupon and the surrounding insulation, as done by Jones et al. (2009). The estimated uncertainty in the extrapolated surface temperature T_s of the test block and the surface heat flux were 1.14 °C and 21.8 kW/m^2, respectively.

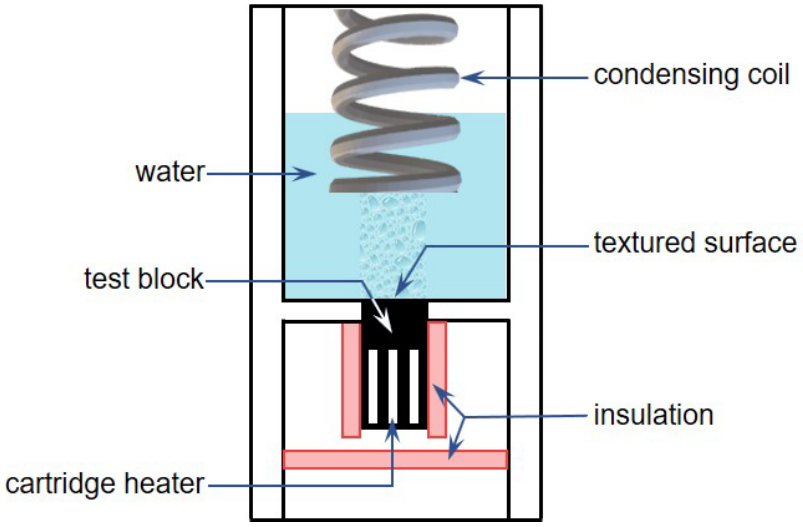

Fig. 3. Experimental setup.

3. Results and discussion

3.1 Boiling performance of EDM surfaces

The first phase of this research focussed on the boiling performance of EDM surfaces with specific reference to the discharge current and the discharge duration. For all surfaces evaluated in this work, the slope and curvature of the boiling curve were calculated, and the surface superheat at which the onset of nucleate boiling (ONB) occurred $\Delta T_{s\text{-}ONB}$ was identified to be the degree of surface superheat ($T_s - T_{sat}$) that corresponds to the maximum curvature. For example, Fig. 4a shows the boiling curve for a reference polished surface of roughness 0.07 µm *Ra*, against which all EDM surfaces were compared; this boiling curve was validated against that

obtained from the Rohsenow correlation for aluminum using a surface factor of 0.012. Fig. 4b and 4c show the slope and curvature of the boiling curve. In this case, $\Delta T_{s\text{-}ONB}$ is equal to 10.1 °C (as indicated by the broken vertical line), which aligns with the 11.0 °C reported by Jones et al. (2009) for a polished surface of 0.04 µm *Ra* roughness.

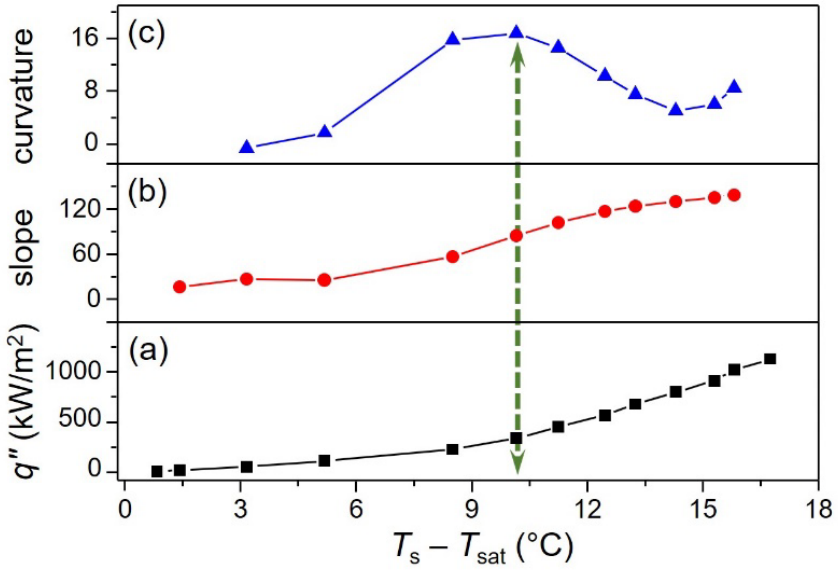

Fig. 4. Demarcation of free convection and boiling regimes.

3.1.1 Effect of discharge current

Fig. 5a and 5b show the effect of discharge current i_e on the boiling performance at a discharge duration t_e of 274 µs that is recommended by the machine tool manufacturer to be optimal for the maximum removal rate in EDM for the aluminum alloy used. An increase in current results in a larger crater size both in terms of its depth and diameter as described by Kunieda et al. (2005), and the investigated discharge currents of 21, 39 and 72 A corresponded to surface roughness values of 18.3, 25.3 and 33.8 µm *Ra*, respectively. It may be noted that such roughness values are an order of magnitude higher than what is typically specified for functional surfaces in

mechanical engineering applications and are in fact not as readily obtained in machining processes other than EDM.

The boiling performance seen in terms of heat flux q'' versus the degree of superheat (T_s - T_{sat}) in Fig. 5a indicates ONB of EDM surfaces at surface temperatures significantly lower than the polished surface. The degree of superheat required for ONB further decreases monotonically with an increase in current, conceivably due to the corresponding increase in the size of nucleating cavities (crater diameter). On examining the heat transfer coefficient h as a function of heat flux q'' (Fig. 5b), for q'' values of about 50 kW/m^2 or lower, the heat transfer coefficients of the polished surface are somewhat higher, pointing to EDM texturing to be of no particular benefit in terms of this metric in this regime. This could be attributed to the obstruction of the buoyancy-driven flow of the fluid by the surface features, and the feature size being larger than the developing thermal boundary layer, which decreases heat transfer from the wall as observed by Nakayama et al. (1980).

At a higher heat flux on the other hand, EDM textured surfaces do perform better. The heat transfer coefficients at a given heat flux are however largely similar, even for a three-fold increase in the discharge current that corresponds roughly to a 100% increase in the *Ra* roughness. The highest current of 72 A, which represents the upper limit for the machine tool used in this work, yielded a modest ~50% improvement in the heat transfer coefficient relative to the polished surface, across the range of heat flux values considered. This is in fact lower than the maximum enhancement obtained using EDM by Jones at al. (2009) by a factor of 2. It may be noted that the maximum heat flux (~1200 kW/m^2) seen in Fig. 5 do not pertain to the critical heat flux, but rather to the limits of the experimental setup.

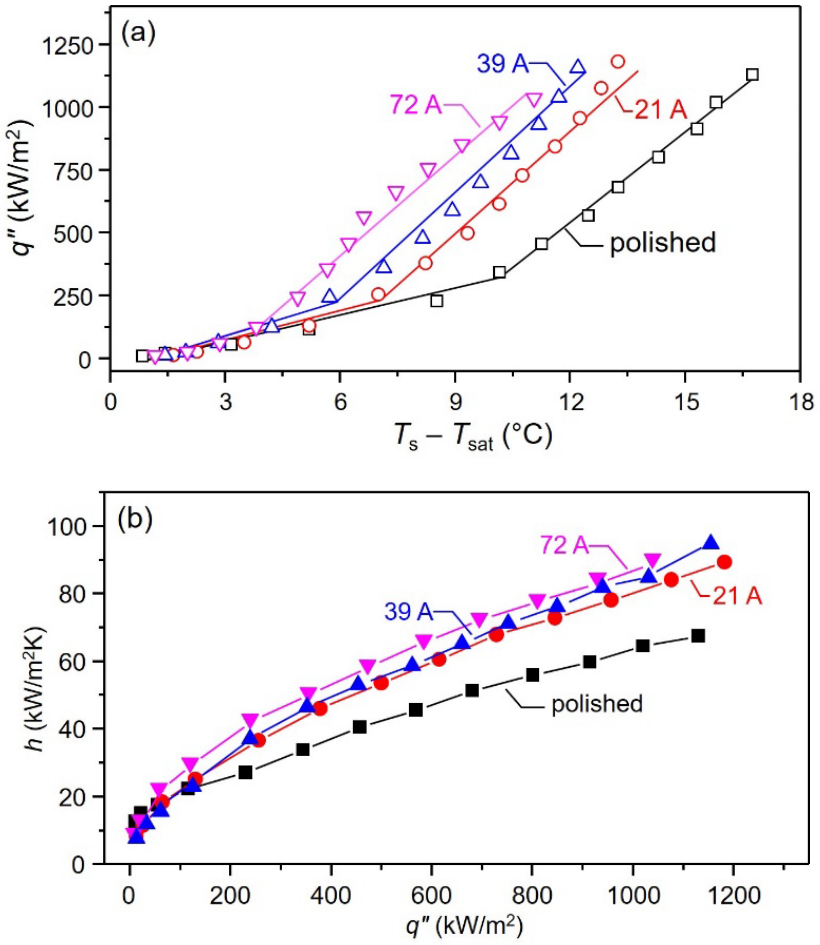

Fig. 5. Effect of discharge current on boiling performance.

3.1.2 Effect of discharge duration

Fig. 6a and 6b show the effect of discharge duration t_e over the range from 65 µs to 6500 µs on the boiling performance of EDM surfaces. Given that the influence of current was shown to be marginal in terms of the heat transfer coefficient enhancement (Fig. 5b), the discharge current was kept constant at 39 A that corresponds to the optimal current density of ~10 A/cm^2 for stable machining in EDM as suggested by Blatnik et al. (2007). The roughness values corresponding to the discharge durations of 65, 274, 1800, 2400, 4200 and 6500 µs were 14.1, 25.3, 41.7, 39.3, 15.5, 17.5 µm *Ra*; in contrast to the discharge current that monotonically increased the roughness, the discharge duration may be noted to exhibit a maximum.

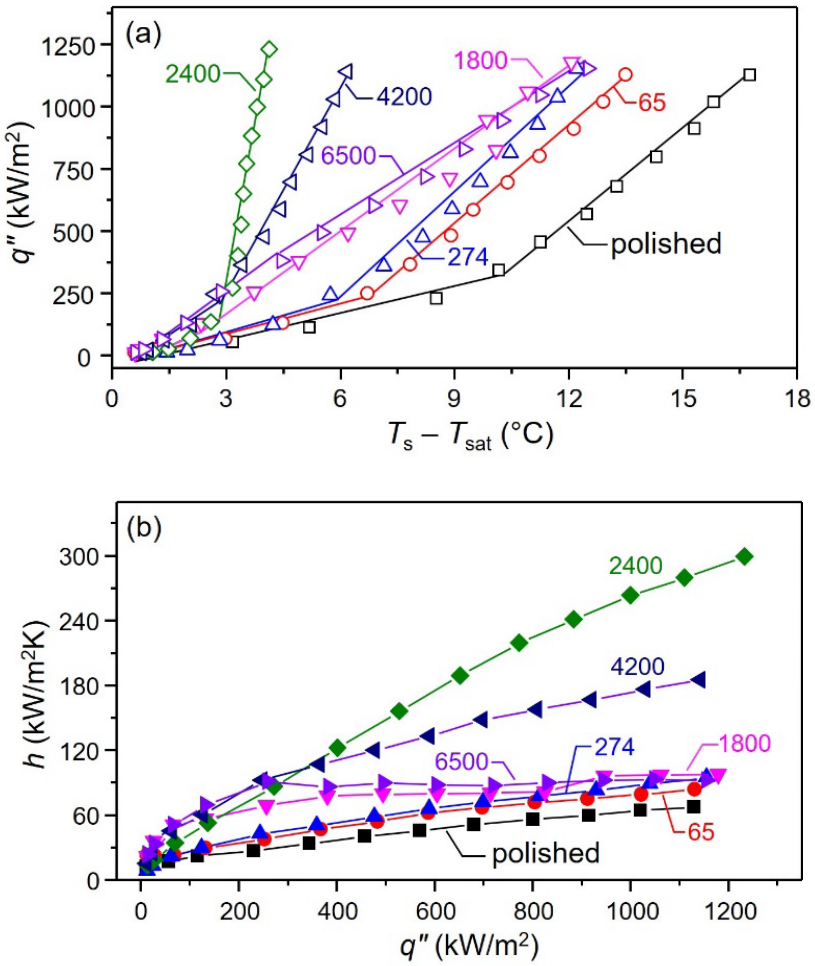

Fig. 6. Effect of discharge duration on boiling performance.

Similar to the effect of discharge current (Fig. 5a), an increase in discharge duration also decreased $\Delta T_{s\text{-}ONB}$ (Fig. 6a) to the extent that $\Delta T_{s\text{-}ONB}$ at the duration of 6500 µs was just 2.8 °C. The convection heat transfer coefficients increased continually with an increase in t_e (Fig. 6b), which agrees with the observation by Rahman and McCarthy (2017) that the Nusselt number increases with an increase in the spacing of surface features. In the nucleate boiling regime, the heat transfer coefficient was initially enhanced notably with an increase in discharge duration (Fig. 6b). This is due to the significant increase in the crater diameter consequent to the expansion of the plasma channel during the duration of the discharge in EDM (Kunieda et al.,

2005), which reduces the incipient superheat. The heat transfer coefficient was however maximized at a discharge duration of 2400 µs (Fig. 6b). At this duration, for a heat flux of 1000 kW/m^2, the enhancement in the heat transfer coefficient was close to 450% of that of the polished surface, which is significantly higher than the 100% increase reported by Jones et al. (2009).

Visual inspection of the machined surface indicated the formation of a superficial layer (Fig. 7a and 7b) with a smaller peak-to-valley surface height (Fig. 7c), developing on the surface at discharge durations higher than 2400 µs. During EDM of Ti, such a layer observed in a study by Holsten et al. (2018) has been identified to be TiC, formed by the reaction of Ti with C derived from the hydrocarbon dielectric fluid. To verify a hypothesis that the formation of the superficial layer was the limiting factor in enhancing boiling heat transfer, EDM texturing was conducted using deionized water as the dielectric fluid instead of the hydrocarbon oil, to prevent possible formation of a carbide that is a thermal barrier (signified by the decrease in roughness, Fig. 7c). Texturing using deionized water as the dielectric did indeed preclude the layer from being formed at all discharge durations. Boiling performance of test surfaces textured in water at a discharge duration of 6500 µs was consequently better than that at 2400 µs (Fig. 8), unlike the ones textured in the hydrocarbon oil, in which case the boiling performance was maximized at 2400 µs (Fig. 6a), beyond which the superficial layer was formed.

Surfaces textured in hydrocarbon oil and deionized water as the dielectric medium corresponded to water contact angles of ~120° and ~20° respectively, as was also reported by Guo et al. (2019). Such a difference in surface wetting was however of no significant influence in terms of boiling performance as shown by Allred et al. (2018), given that the water was degassed before

283 the boiling experiments using immersion heaters; in such a case, any air trapped within the
284 interstices of the textured surface would diffuse into the water and be subsequently removed.
285 This did ensure that the test surfaces were wetted in the Wenzel state (wherein the water intrudes
286 into the interstices to correspond to a homogenous wetted interface) and not the Cassie-Baxter
287 state (which is a composite solid-air-liquid interface), and the differences in boiling performance
288 may indeed be attributed to the surface topography rather than their wettability.

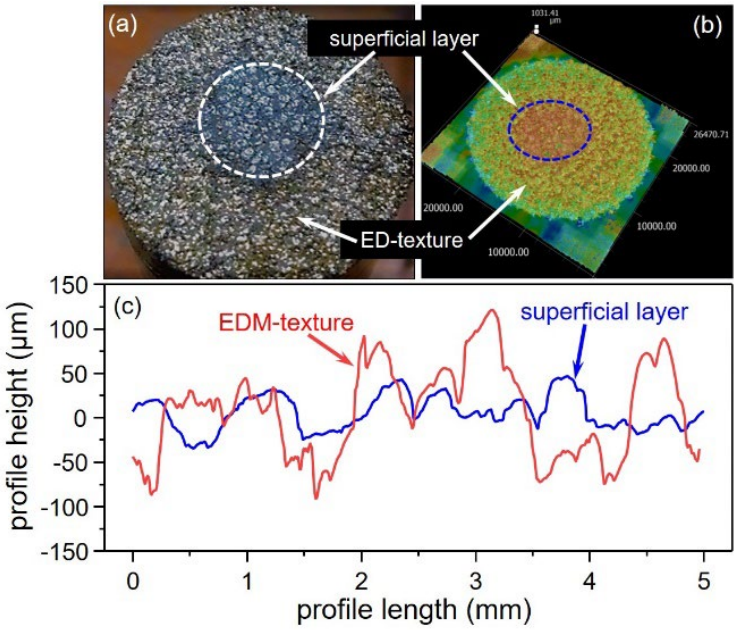

289 *Fig. 7. Formation of a superficial layer on EDM surface.*

290 Having identified the formation of the superficial layer to be the limiting factor that inhibits
291 boiling heat transfer, further experiments were conducted to understand the relevant
292 mechanisms. Noting that the areal extent of the layer increased with the machining duration,
293 boiling experiments were conducted using test blocks which corresponded to machining times of
294 30, 400 and 900 s at a discharge current of 39 A and a discharge duration of 2400 µs. Insets in
295 Fig. 9 indicate little to no layer formation at machining time of 30 s. The area over which the

superficial layer is formed increased as the machining time is further increased from 400 s to 900 s. Such layer formation was found to decrease the $\Delta T_{s\text{-}ONB}$ from 2.8 °C at 30 s to about 1.5 °C at 400 s and 900 s, and to enhance heat transfer in the natural convection regime. As the roughness decreases with the deposition of the layer as shown in Fig. 7c, the enhancement in this regime is possibly due to the reduced obstruction to buoyancy-driven flows, as previously alluded to.

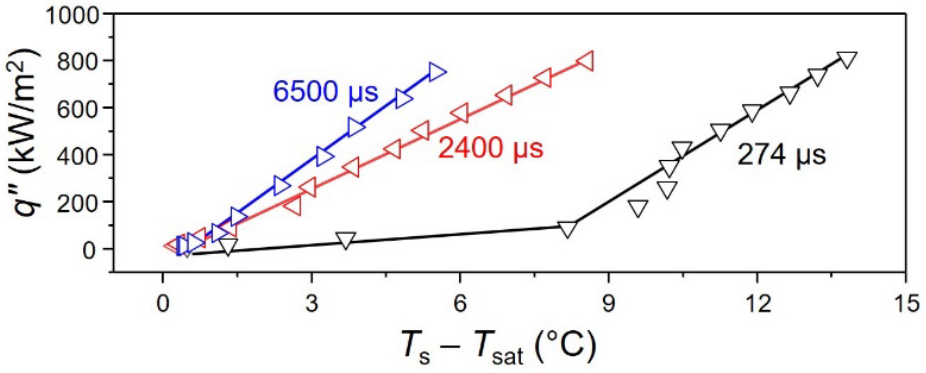

Fig. 8. Boiling performance of surfaces generated in water.

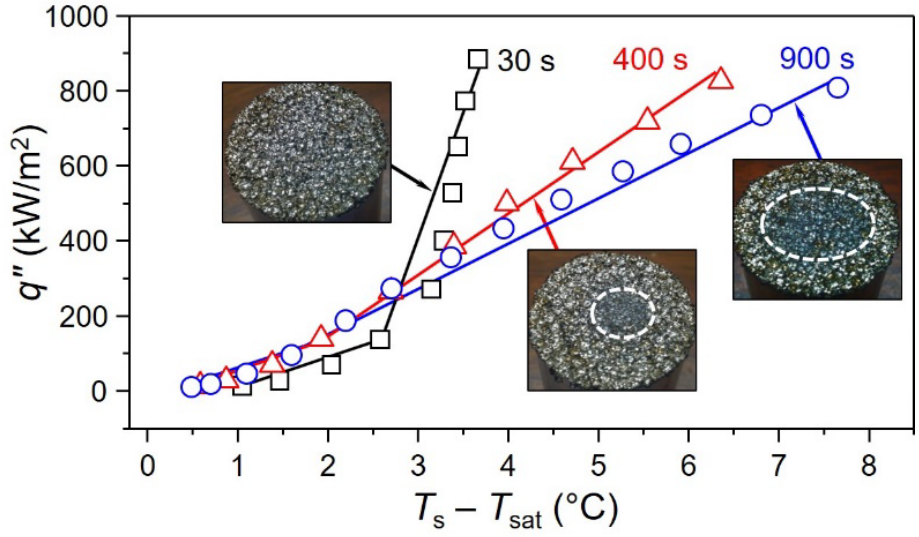

Fig. 8. Influence of surface layer on boiling performance.

Bubble nucleation and bubble growth were examined off surfaces textured for different machining times at surface superheats of 1.5, 2.5 and 3.5 °C using high-speed imaging (Fig. 10).

306 It was observed that nucleation was initiated at a higher degree of superheat for the surface that
307 had no superficial layer (machining time of 30 s) and boiling was the most vigorous for this
308 surface. At a surface superheat of 3.5 °C, this surface was in the fully-developed nucleate boiling
309 regime, with bubbles merging horizontally and growing in the form of slugs and columns, as
310 indicated by the images shown in the top row of Fig 10.

311 Many relatively smaller bubbles were observed to depart from surfaces with the superficial layer
312 (machining time of 400 s and 900 s), as shown in the second and third rows of Fig 10. Bubble
313 departure size depends on forces acting on a bubble during the growth process as described by
314 Jones et al. (2009). The formation of the superficial layer seems to affect such a force balance
315 and reduce bubble departure size. Furthermore, the deposited layer reduced the number of active
316 nucleation sites, hence reducing nucleate boiling behaviour. Additional insights into the role of
317 the superficial layer may be gained by more extensive investigations into bubble dynamics,
318 which was beyond the scope of the present work.

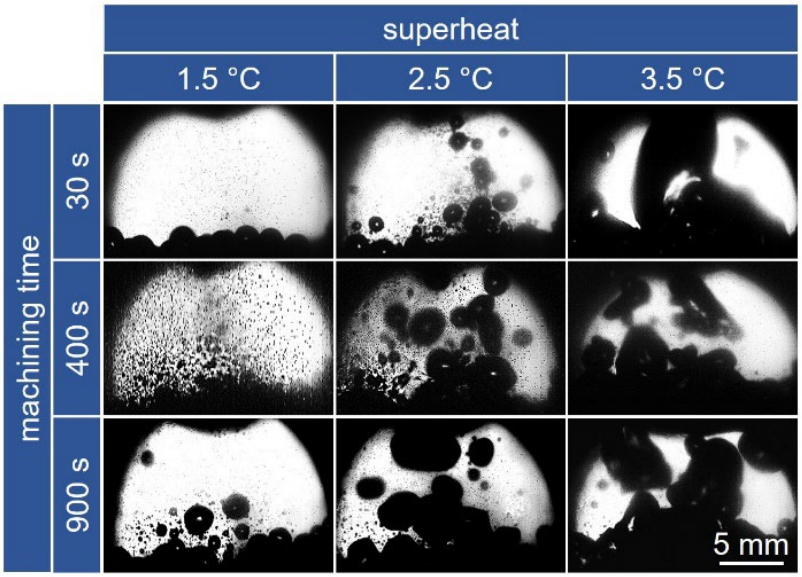

319 *Fig. 9. Bubble nucleation and growth.*

3.1.3 Comparison with research elsewhere

To gain a perspective on the relative boiling performance of EDM surfaces, the pool boiling curve corresponding to the surface with the best boiling performance from the present work (discharge current i_e 72 A, discharge duration t_e 2400 µs, machining time 30 s, hydrocarbon dielectric fluid) was compared against those from other boiling enhancement techniques reported in the literature (Fig. 11).

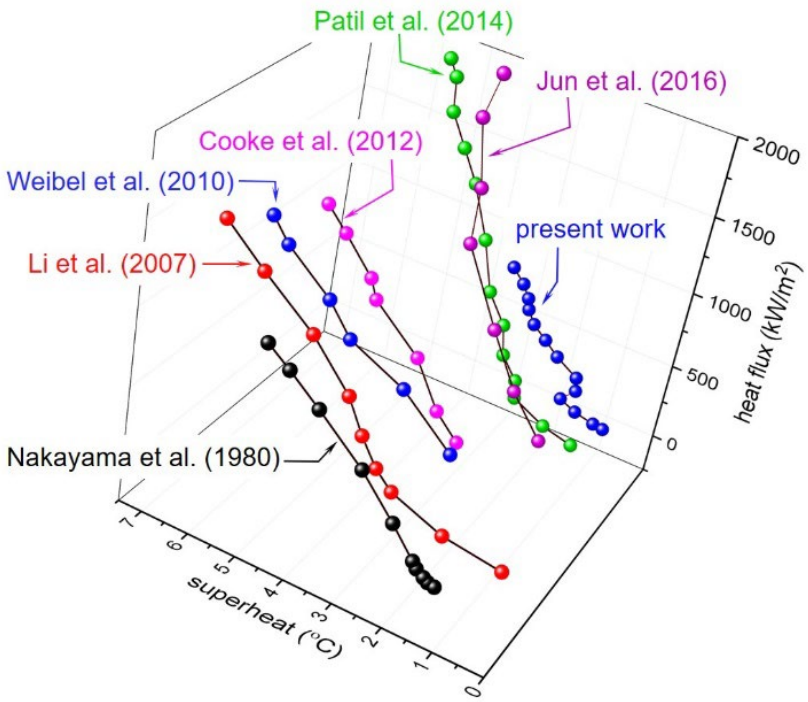

Fig. 10. Comparison of boiling curves.

The best boiling performance from the present work is comparable to that from Patil and Kandlikar (2014) who used electrodeposition over fin tops of microchannels, and that from Jun et al. (2016) who used sintered copper microporous coatings. The authors in these two studies reported a heat transfer coefficient h of 995 kW/m^{2}K at a surface heat flux of 2480 kW/m^2 and a surface superheat of 2.5 °C, and 400 kW/m^{2}K at a heat flux of 2025 kW/m^2 and a surface

332 superheat of 5 °C, respectively. The present work referred to a maximum *h* of 237 kW/m^{2}K at a
333 heat flux of 1080 kW/m^2 at a wall superheat of 3.4 °C. The best EDM surface can likely
334 correspond to a higher *h* with a further increase in the wall heat flux, which was unfortunately
335 not realizable in the present experimental setup. An investigation on the critical heat flux of
336 EDM surfaces is warranted to quantify the maximum *h* attainable. The performance was
337 significantly better than the boiling enhancement techniques reported by Cooke and Kandlikar
338 (2012), Weibel et al. (2010), Li and Peterson (2007) and Nakayama et al. (1980). The capability
339 of EDM in terms of rapidly and repeatability texturing any electrically conducting material
340 irrespective of mechanical properties, towards significantly enhancing its boiling performance,
341 renders it worthy of consideration vis-à-vis the other techniques above.

342 *3.2 Correlation of roughness indices to boiling performance*

343 Many investigations on pool boiling heat transfer rely on the average roughness *Ra*. Correlations
344 based on *Ra* have had limited success in instances such as Vachon et al. (2013) or have been
345 found to be rather weak in the work of Jabardo (2010), Kim et al. (2008), and Chowdhury and
346 Winterton (1985). However, some researchers like Jones et al. (2009) have been able to correlate
347 the general trend of increasing heat transfer coefficients with increased roughness. In this
348 context, the present work attempted to correlate nucleate boiling heat transfer of EDM surfaces
349 to conventional roughness parameters such as *Ra*, the root mean square deviation of the profile
350 *Rq*, the maximum height of the profile *Rz*, and the skewness *Rsk* and kurtosis *Rku*.

351 In addition, a mechanistic approach has been also adopted to correlate nucleate boiling heat
352 transfer of EDM surfaces to surface geometric parameters (e.g., crater diameter C_d, crater height

353 C_h and crater volume V_c) that refer to characteristic EDM craters obtained by using the Data
354 Dependent System (DDS) approach. DDS is a methodology that mathematically models the
355 superimposition of several overlapping craters that pertain to random depths and locations to
356 generate the composite EDM surface. Accordingly, a characteristic crater may be computed
357 directly from the measured surface profile that corresponds to a specific machining condition
358 (discharge duration and current in the present case) using the approach outlined by Pandit and
359 Rajurkar (1980).

360 The correlation analysis entailed EDM surfaces with a roughness in the range of 14 μm to 70 μm
361 *Ra*. The heat transfer coefficient *h* in the nucleate boiling regime was correlated to the surface
362 characteristic index *Z* in the form $h = AZ^B$, and the coefficients A and B were obtained by
363 regression. Fig. 12 shows two of the lowest Mean Absolute Error (MAE) values to refer to the
364 crater diameter C_d (13.1%) and the crater volume V_c (14.9%) obtained using the DDS
365 methodology. This is in alignment with the knowledge that cavities with a larger mouth diameter
366 need a smaller superheat to nucleate bubbles. It is further possible that wider craters lead to the
367 separation of the flow of liquid and vapor, which induces efficient heat transfer through better
368 convection as observed by Patil and Kandlikar (2014). Likewise, an increase in crater volume
369 refers to trapping of more vapor volume during the initial wetting stage.

370 Conventional roughness parameters *Ra* (17.6%) and *Rq* (17.8%) that showed similar correlation
371 performance referred to the two next higher correlation errors. This shows that it is expedient to
372 use the *Ra* and *Rq* parameters that are readily obtained from commercial surface profilers to
373 correlate boiling performance, especially when surfaces being compared pertain to the same
374 manufacturing process (EDM in this case). At the same time, it does but also highlight the value

in adopting parameters such as the crater diameter and volume that are physically meaningful in the context of boiling physics, which can be mathematically extracted from the corresponding surface profiles using the DDS methodology for somewhat lower correlation errors. It is interesting to note that the crater height C_h (24.1%) and the maximum height of the profile *Rz* (25.1%), which are both amplitude parameters, correspond to a similar correlation error (Fig 12). The skewness *Rsk* and kurtosis *Rku* parameters carried even higher errors of 26.6% and 38.4%, respectively.

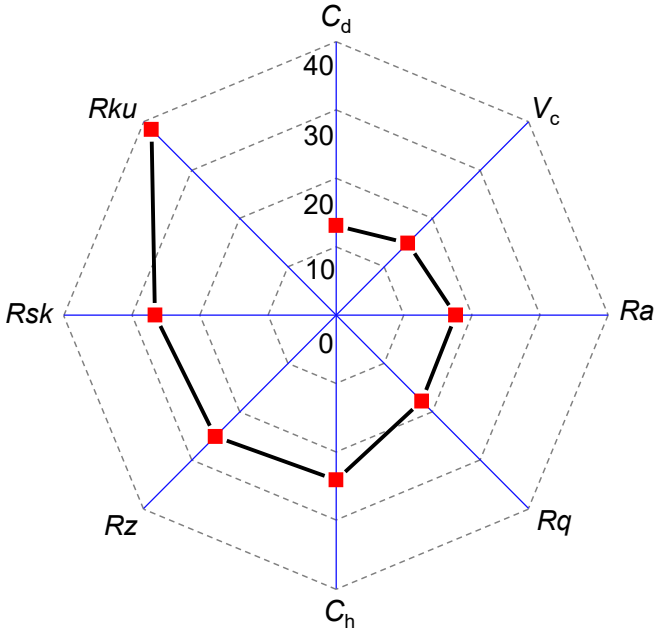

Fig. 11. Mean Absolute Error (%) on correlating heat transfer coefficient h to various surface indices.

4. Conclusions

An experimental study has been carried out to assess the level of enhancement in boiling performance brought about through texturing Aluminium 6061 alloy surfaces using sink

electrical discharge machining, by systematically varying the discharge current and discharge duration. While the discharge current indicated a monotonic increase in performance over the range investigated, the discharge duration exhibited an optimum, due to the formation of a superficial layer during machining that was facilitated by the hydrocarbon dielectric used in the process. A maximum heat transfer coefficient of 237 kW/m^2K at a surface superheat ΔT_{sat} = 3.4 °C was obtained when texturing at a discharge current of 72 A and a discharge duration of 2400 µs when using a hydrocarbon dielectric. This roughly represents a five-fold enhancement in boiling performance relative to a reference polished surface, which highlights the significant potential of sink EDM for enhancing pool boiling performance.

EDM surfaces were characterized using conventional roughness parameters such as *Ra*, *Rq* and *Rz* to correlate their boiling performance. A methodology known as Data Dependent Systems was also invoked to mathematically extract geometrical parameters referring to characteristic craters that collectively constitute the surface, for correlating surface topography and boiling performance. Among these two classes, the average roughness parameter *Ra* and the diameter of the characteristic crater were found to offer the best correlations with largely comparable correlation errors.

Acknowledgements

This work was funded by Discovery and Strategic Network (Canadian Network for Research and Innovation in Machining Technology) Grants from the Natural Sciences and Engineering Research Council of Canada, and Pratt & Whitney Canada.

References

Ahmed, N., Murray, J.W., Yuzawa, T., Nakagawa, T., Sarugaku, S., Saito, D., Brown, P.D., Clare, A.T., 2020. Formation of thick electrical discharge coatings, Journal of Materials Processing Technology 285, 116801. https://doi.org/10.1016/j.jmatprotec.2020.116801.

Ahmed, O., Hamed, M., 2012. Effect of nanoparticle deposition on pool boiling of nanofluids, International Journal of Heat and Mass Transfer 55, 3423–3436. https://doi.org/10.1016/j.ijheatmasstransfer.2012.02.021.

Allred, T., Weibel J., Garimella S., 2018. Enabling highly effective boiling from superhydrophobic surfaces, Physical Review Letters 120, 174501. https://doi.org/10.1103/PhysRevLett.120.174501

Bangash, MK, Casalegno, V, Das, AK, Ambrois, SP, Ferraris, M., 2020. Surface machining of Ti6Al4V by means of Micro-Electrical Discharging to improve adhesive joining, Journal of Materials Processing Technology 286, 116813. https://doi.org/10.1016/j.jmatprotec.2020.116813.

Blatnik, O., Valentincic, J., Junkar, M., 2007. Percentage of harmful discharges for surface current density monitoring in electrical discharge machining process, Journal of Engineering Manufacture 221, 1677–1684. https://doi.org/10.1243/09544054JEM816.

Chowdhury, S., Winterton, R., 1985. Surface effects in pool boiling, International Journal of Heat and Mass Transfer 28, 1881–1889. https://doi.org/10.1016/0017-9310(85)90210-8.

Cooke D., Kandlikar, S., 2012. Effect of open microchannel geometry on pool boiling enhancement, International Journal of Heat and Mass Transfer 55, 1004–1013. https://doi.org/10.1016/j.ijheatmasstransfer.2011.10.010.

Dhadda G., 2019. Pool boiling heat transfer enhancement with sink electrical discharge machined surfaces, Masters Thesis, McMaster University, Canada. https://macsphere.mcmaster.ca/handle/11375/26153

Giesler, K., Bar-Cohen, A., 2005. Surface effects on confinement-driven pool boiling enhancement in vertical parallel-plate channels, ASME Summer Heat Transfer Conference, San Francisco, 195–205. https://doi.org/10.1115/HT2005-72666.

Guo, C., Koshy, P., Coelho, F., Selvaganapathy, P., 2019. Sink electrical discharge machining of hydrophobic surfaces, CIRP Annals 68, 185–188. https://doi.org/10.1016/j.cirp.2019.04.101.

Holsten, M., Koshy, P., Klink, A., Schwedt, A., 2018, Anomalous influence of polarity in sink EDM of titanium alloys, CIRP Annals 67, 221–224. https://doi.org/10.1016/j.cirp.2018.04.069.

Jabardo, J., 2010. An overview of surface roughness effects on nucleate boiling heat transfer, The Open Transport Phenomena Journal 2, 35–47. http://dx.doi.org/10.2174/1877729501002010035

447 Jones, B., McHale, J., Garimella, S., 2009. The influence of surface roughness on nucleate pool
448 boiling heat transfer, Journal of Heat Transfer 131, 121009:1–13.
449 https://doi.org/10.1115/1.3220144.

450 Jun, S., Kim, J., Son, D., Kim, H., You, S., 2016. Enhancement of pool boiling heat transfer in
451 water using sintered copper microporous coatings, Nuclear Engineering and Technology 48,
452 932–940. https://doi.org/10.1016/j.net.2016.02.018.

453 Kim, J., Park, B., Lee, J., 2008. Natural convection heat transfer around microfin arrays,
454 Experimental Heat Transfer 21, 55–72. https://doi.org/10.1080/08916150701647835.

455 Kunieda, M., Lauwers, B., Rajurkar, K., Schumacher, B., 2005. Advancing EDM through
456 fundamental insight into the process, CIRP Annals 54, 64–87. https://doi.org/10.1016/S0007-
457 8506(07)60020-1.

458 Li, C., Peterson, G., 2007. Parametric Study of pool boiling on horizontal highly conductive
459 microporous coated surfaces, Journal of Heat Transfer 129, 1465–1475.
460 https://doi.org/10.1115/1.2759969.

461 Liang, G., Mudawar, I., 2019. Review of pool boiling enhancement by surface modification,
462 International Journal of Heat and Mass Transfer 128, 892–933.
463 https://doi.org/10.1016/j.ijheatmasstransfer.2018.09.026.

464 Nakayama, W., Daikoku, T., Kuwahara, H., Nakajima, H., 1980. Dynamic model of enhanced
465 boiling heat transfer on porous surfaces—Part I: experimental investigation, Journal of Heat
466 Transfer 102, 445–450. https://doi.org/10.1115/1.3244320.

467 Nirgude, V., Sahu, S., 2017. Enhancement of nucleate boiling heat transfer using structured
468 surfaces, Chemical Engineering and Processing: Process Intensification 122, 222–234.
469 https://doi.org/10.1016/j.cep.2017.10.013.

470 Pandit, S., Rajurkar, K., 1980. Crater geometry and volume from electro discharge machined
471 surface by Data Dependent Systems, Journal of Engineering for Industry 102 (1980) 289–295.
472 https://doi.org/10.1115/1.3183867.

473 Patil, C., Kandlikar, S., 2014. Pool boiling enhancement through microporous coatings
474 selectively electrodeposited on fin tops of open microchannels, International Journal of Heat and
475 Mass Transfer 79, 816–828. https://doi.org/10.1016/j.ijheatmasstransfer.2014.08.063.

476 Rahman, M., McCarthy, M., 2017. Effect of length scales on the boiling enhancement of
477 structured copper surfaces, Journal of Heat Transfer 139, 111508:1–9.
478 https://doi.org/10.1115/1.4036693.

479 Stout, K., Davis, E., Sullivan, P., 1990. Atlas of Machined Surfaces, Chapman and Hall, London.

Vachon, R., Tanger, G., Davis, D., and Nix, G., 2013. Pool boiling on polished and chemically etched stainless-steel surfaces, Journal of Heat Transfer, 231–238. https://doi.org/10.1115/1.3597486.

Weibel, J., Garimella, S., and North, M., 2010. Characterization of evaporation and boiling from sintered powder wicks fed by capillary action, International Journal of Heat and Mass Transfer 53, 4204–4215. https://doi.org/10.1016/j.ijheatmasstransfer.2010.05.043.

List of figures